CP asymmetry in $b \to s l^+ l^-$ decay

T. M. Aliev,* D. A. Demir, E. Iltan, and N. K. Pak
Physics Department, Middle East Technical University, Ankara, Turkey
(Received 13 November 1995)

Using the experimental upper bound on the neutron electric dipole moment and the experimental result on the $b \to s\gamma$ branching ratio we have calculated the *CP* asymmetry and $\Gamma^{2HDM}(b \to s l^+ l^-)/\Gamma^{SM}(b \to s l^+ l^-)$. It is shown that in the invariant dilepton mass q^2 region $(m_{\psi'}^2 + 0.2\ \mathrm{GeV}^2) < q^2 < m_b^2$ the *CP* asymmetry is maximal and quite detectable. [S0556-2821(96)02211-4]

PACS number(s): 11.30.Er, 12.60.Fr, 13.20.He

I. INTRODUCTION

The experimental discovery of the inclusive and exclusive decays $B \to X_s\gamma$ and $B \to K^*\gamma$ by the CLEO Collaboration [1,2] has triggered a lot of theoretical and experimental activity in the field of rare decays of B mesons. These decays are interesting for checking the predictions of the standard model (SM) at the one-loop level, for determining the Cabibbo-Kobayaski-Mastawa (CKM) matrix elements, and for looking for the ''new physics'' beyond the SM. From the experimental point of view another promising decay in this direction is the semileptonic decay $b \to X_s l^+ l^-$, because this decay is easier to measure provided that we are given a good electromagnetic detector and a large number of B hadrons. Theoretically this decay has been the subject of many works in the framework of the SM [3–6] and its extensions, particularly in the two Higgs doublet model (2HDM).

$b \to s l^+ l^-$ decay is a flavor-changing neutral current (FCNC) process which appears only at the one- loop level of pertubation theory. The basic thing about this decay is that the penguin diagrams provide the two key ingredients needed for partial rate asymmetries. Being a loop diagram, it involves all three generations, each generation contributing with different elements of the CKM matrix. At the same time the loop effects that involve on-shell particle rescatterings provide the necessary absorbtive parts.

It is well known that in the 2HDM, the $b \to s l^+ l^-$ decay receives significant contributions from the charged Higgs boson ($H^\pm$) exchange [7]. Another interesting pecularity of the 2HDM is the appearence of new sources of *CP* violation [8] in addition to the one in the SM. An interesting version of the 2HDM, the so-called most general 2HDM, which was proposed in [9], has a new source of *CP* violation, arising from the relative phase between the vacuum expectation values of two Higgs scalars.

In this work we shall work out the $b \to s l^+ l^-$ decay. In particular we shall determine the *CP* asymmetry A and the ratio $r = \Gamma^{2HDM}(b \to s l^+ l^-)/\Gamma^{SM}(b \to s l^+ l^-)$ as functions of the charged Higgs mass.

In the calculation of the *CP* asymmetry we shall consider both the SM and 2HDM contributions simultaneously. In determining r and A we shall make use of the experimental results on $B(b \to s\gamma)$ [1,2], and the neutron electric dilpole moment (EDM).

Section II is devoted to the derivation of basic theoretical results and Sec. III contains the numerical analysis of them.

II. FORMALISM

In the most general 2HDM [8,9] the couplings of $H^\pm$ with t_R and b_R is characterized by the coefficients ξ_f defined by

$$\xi_f = \frac{\sin\delta_f}{\sin\beta\cos\beta\sin\delta} e^{i\sigma_f(\delta - \delta_f)} - \cot\beta, \tag{1}$$

where $f = t$ or b, $\sigma_f = +$ for b and $-$ for t, and $\delta_f = h_2/h_1$ where h_2 and h_1 are the diagonal elements of the matrices Γ_2^u and Γ_1^u, respectively. Here Γ^u are the matrices in the flavor space, and determine the Yukawa couplings (for more details see [9]), and δ is the relative phase between the vacuum expectations of the two Higgs scalars:

$$\langle \phi_1^0 \rangle = \frac{v}{\sqrt{2}} \cos\beta e^{i\delta}, \quad \langle \phi_2^0 \rangle = \frac{v}{\sqrt{2}} \sin\beta. \tag{2}$$

The most general 2HDM reduces to the well-known 2HDM's in the current literature, in certain limiting cases [9]. Namely, if $\delta_t = \delta_b = 0$, then $\xi_t = \xi_b = -\cot\beta$ (model I) and, if $\delta_b = \delta, \delta_t = 0$, then $\xi_t = -\cot\beta, \xi_b = \tan\beta$ (model II).

As mentioned above the penguin diagrams provide the necessary absorbtive parts for the calculation of the *CP* asymmetry. In this decay the dilepton invariant mass q^2 ranges from $4m_l^2$ to m_b^2 therefore, the u and c loops give rise to nonzero absorbtive parts which are described, at the point $\mu = m_b$, by

$$F = i4\sqrt{2} G_F \lambda_u \frac{\alpha}{4\pi} A_9 \overline{s_L} \gamma_\mu b_L l^+ \gamma_\mu l^-, \tag{3}$$

where $\lambda_i = V_{is} V_{ib}^*$ and the function A_9 is given by

$$A_9 = w_u [Q(m_c^2/q^2) - Q(m_u^2/q^2)], \tag{4}$$

where

$$Q(x) = \frac{2\pi}{9}(2 + 4x)\sqrt{1 - 4x}\,\theta(1 - 4x) \tag{5}$$

*Permanent address: Institute of Physics, Azerbaijanian Academy of Sciences, Baku, Azerbaijan.

and w_u, having the numerical value of 0.3864, comes from the renormalization group equation (RGE) movement of the Wilson coefficients from the $\mu=M_W$ to $\mu=m_b$ point.

It is well known that in the range $(4m_l^2, m_b^2)$ one can create real low lying charmonium states [10,11]. In this work we shall discard that portion of total dilepton mass range including the J/ψ and ψ' poles and the region between them to avoid the addition of new hadronic uncertainities to the decay amplitude. Thus we restrict ourselves to the following kinematical regions [6]:

$$\text{region I:} \quad 4m_l^2 \leqslant q^2 \leqslant (m_\psi^2 - \tau),$$

$$\text{region II:} \quad (m_{\psi'}^2 + \tau) \leqslant q^2 \leqslant m_b^2, \tag{6}$$

where $\tau = 0.2\ \text{GeV}^2$ is the cutoff parameter.

Taking into account the 2HDM contributions and absorbtive part described by F in (3), the amplitude for $b \to s l^+ l^-$ can be written as

$$M_{b\to s l^+ l^-} = 4\sqrt{2} G_F \frac{\alpha}{4\pi} \Big(C_9^{\text{eff}}(\mu) \overline{s_L} \gamma_\mu b_L l^+ \gamma_\mu l^- + C_{10}(\mu) \overline{s_L} \gamma_\mu b_L l^+ \gamma_\mu \gamma_5 l^- + \frac{q^\nu}{q^2} \times C_7(\mu) \overline{s} \sigma_{\mu\nu} (m_b R + m_s L) b l^+ \gamma_\mu l^- \Big). \tag{7}$$

The Wilson coefficients appearing in (7) are given by

$$C_7(\mu) = \lambda_t [C_7^{\text{SM}}(\mu) + C_7^{\text{2HDM}}(\mu)],$$

$$C_9^{\text{eff}}(\mu) = \lambda_t [C_9^{\text{SM}}(\mu) + C_9^{\text{2HDM}}(\mu)] + i\lambda_u A_9,$$

$$C_{10}(\mu) = \lambda_t [C_{10}^{\text{SM}}(\mu) + C_{10}^{\text{2HDM}}(\mu)]. \tag{8}$$

The explicit forms of $C_i^{\text{SM}}(\mu)$ $(i=7,9,10)$ including leading and next-to-leading order QCD corrections can be found in [3,12–14]. The 2HDM contributions, $C_i^{\text{2HDM}}(\mu)$, in the framework of the most general 2HDM [9] are given by

$$C_7^{\text{2HDM}}(\mu) = |\xi_t|^2 K_7^{tt} + (R_{tb} + iI_{tb}) K_7^{tb},$$

$$C_9^{\text{2HDM}}(\mu) = |\xi_t|^2 K_9^{tt},$$

$$C_{10}^{\text{2HDM}}(\mu) = |\xi_t|^2 K_{10}^{tt}, \tag{9}$$

where $R_{tb} = \text{Re}[\xi_t \xi_b^*], I_{tb} = \text{Im}[\xi_t \xi_b^*]$, and

$$K_7^{tb} = \eta^{16/23} [G(y) - \tfrac{8}{3}(1 - \eta^{-2/23}) E(y)],$$

$$K_7^{tt} = \tfrac{1}{6}\, \eta^{16/23} [A(y) + \tfrac{8}{3}(1 - \eta^{-2/23}) D(y)],$$

$$K_9^{tt} = -\frac{-1 + 4s_W^2}{s_W^2} \frac{x}{2} B(y) + yF(y),$$

$$K_{10}^{tt} = -\frac{1}{s_W^2} \frac{x}{2} B(y), \tag{10}$$

with $x = m_t^2/M_W^2$, $y = m_t^2/M_H^2$, $s_W^2 = 0.2315$, $\eta = \alpha_s(M_W)/\alpha_s(m_b)$ and the explicit expressions for functions A, B, D, E, F, G can be found in [12].

As noted in [9], ξ_t is expected to be of order of unity or less, if the Yukawa couplings of the top quark is reasonable. We have shown that this happens to hold also for the decay process under consideration. Thus, without loosing generality, in what follows we set $|\xi_t|^2 = 0$ (all the conclusions remain in force for the case of $|\xi_t|^2 = 1$ as well).

Using (7), the differential decay rate for $b \to s l^+ l^-$ is obtained as

$$\frac{d\Gamma^{\text{2HDM}}}{ds} = \lambda_0 (1-s)^2 \Big[4 \Big(\frac{2}{s} + 1 \Big) \Big| C_7(\mu) \Big|^2 + (1+2s) \times [|C_9^{\text{eff}}(\mu)|^2 + |C_{10}(\mu)|^2] + 12\,\text{Re}[C_7(\mu) C_9^{\text{eff}}(\mu)] \Big], \tag{11}$$

where $s = q^2/m_b^2$, and $\lambda_0 = \alpha^2 G_F^2 / 768\pi^5$.

After integrating (11) over s we get

$$\gamma = \gamma_0 + 4\rho I^2 + 2I(6I_9 + 6a_9^{(1)} R_{tu}) + 4\rho R^2 + 2R(6R_9 + 6a_9^{(1)} I_{tu} + 4\rho C_7^{\text{SM}}) + 12 a_9^{(1)} C_7^{\text{SM}} I_{tu} + a_9^{(2)} f_{tu} + 2(a_{r9} I_{tu} + a_{i9} R_{tu}), \tag{12}$$

where

$$\gamma = \frac{\Gamma^{\text{2HDM}}}{\lambda_0 |\lambda_t|^2}, \quad \gamma_0 = \left(\frac{\Gamma^{\text{SM}}}{\lambda_0 |\lambda_t|^2} \right) \Big|_{A_9 = 0}, \quad I = I_{tb} K_{tb}^7,$$

$$R = R_{tb} K_{tb}^7, \quad I_{tu} = \frac{\text{Im}[\lambda_t \lambda_u^*]}{|\lambda_t|^2},$$

$$R_{tu} = \frac{\text{Re}[\lambda_t \lambda_u^*]}{|\lambda_t|^2}, \quad f_{tu} = \frac{|\lambda_u|^2}{|\lambda_t|^2}, \tag{13}$$

and the other parameters in (12) are defined by the following integrals:

$$\rho = \int ds (1-s)^2 \Big(\frac{2}{s} + 1 \Big), \quad R_9 = \int ds (1-s)^2 \text{Re}(C_9^{\text{SM}}),$$

$$I_9 = \int ds (1-s)^2 \text{Im}(C_9^{\text{SM}}), \quad a_9^{(1)} = \int ds (1-s)^2 A_9,$$

$$a_9^{(2)} = \int ds (1-s)^2 (1+2s) A_9^2,$$

$$a_{r9} = \int ds (1-s)^2 (1+2s) \text{Re}(C_9^{\text{SM}}) A_9,$$

$$a_{i9} = \int ds (1-s)^2 (1+2s) \text{Im}(C_9^{\text{SM}}) A_9. \tag{14}$$

For the CP conjugate process, the analog of (12) can be obtained by the following replacements:

$$\overline{\gamma} = \gamma (I \to -I; \quad I_{tu} \to -I_{tu}). \tag{15}$$

Now we introduce the parameter r that measures the relative strength of 2HDM and SM rates

$$r=\frac{\gamma}{\gamma_{\rm SM}}, \tag{16}$$

where $\gamma_{\rm SM}$ is obtained by setting $I=R=0$ in (12).

Next we define the CP asymmetry by

$$A=\frac{\overline{\gamma}-\gamma}{\overline{\gamma}+\gamma}. \tag{17}$$

Substituting the expressions for γ and $\gamma_{\rm SM}$ into (16) we obtain a circle for fixed values of r:

$$(R+R_0)^2+(I+I_0)^2=t(r-1)+R_0^2+I_0^2, \tag{18}$$

where the parameters R_0 and I_0 are given by

$$R_0=\frac{3}{2\rho}\left(R_9+\frac{2}{3}\rho C_{\rm SM}^7\right)+r_0,$$

$$I_0=\frac{3}{2\rho}(I_9+a_9^{(1)}R_{tu}), \tag{19}$$

and the quantity $r_0=(3/2\rho)a_9^{(1)}I_{tu}$ is introduced for later use.

On the other hand, insertion of (12) and (15) into (17) yields another circle

$$(R+R_0')^2+(I+I_0')^2=-t+\epsilon\left(1-\frac{1}{A}\right)+R'^2_0+I'^2_0, \tag{20}$$

where

$$I_0'=\frac{I_0}{A},\quad R_0'=\frac{3}{2\rho}\left(R_9+\frac{2}{3}\rho C_7^{\rm SM}\right)+\frac{r_0}{A}. \tag{21}$$

The parameters ϵ and t in (19) and (20) are given by

$$\epsilon=\frac{I_{tu}}{4\rho}(12a_9^{(1)}C_7^{\rm SM}+2a_{r9}),$$

$$t=-\frac{1-A_s}{A_s}\epsilon, \tag{22}$$

where A_s is the CP asymmetry in SM which is obtained from (17) by

$$A_s=A|_{I=R=0}. \tag{23}$$

Note that the CP asymmetry in SM has previously been studied in [15]. Up to this point, our analysis of $b\to sl^+l^-$ decay parallels that of $b\to s\gamma$ in [9] except for the definition of A. We shall, however, analyze the circles in (18) and (20) in a different context by exploiting the relation between I and neutron EDM, and experimental results on $b\to s\gamma$ branching ratio [1,2].

First we obtain the expression for the CP asymmetry in (17) by subtracting (20) from (18) and solving for A:

$$A=\frac{1}{1-a}, \tag{24}$$

where

$$a=\frac{\rm tr}{\epsilon+2II_0+2Rr_0}. \tag{25}$$

Now we turn to the determination of I with the use of the experimental upper bound on neutron EDM. Weinberg has proposed a CP violating six-dimensional gluonic operator [16]

$$O_6\sim f_{abc}G_a^{\mu\rho}G_{b\rho}^{\nu}\widetilde{G}_{c\mu\nu}, \tag{26}$$

which has been shown to give very large contribution to neutron EDM, d_n by the neutral [16] or charged [17] Higgs exchange. Weinberg, after relating the hadronic matrix elements of O_6 to d_n, predicts the value of d_n on the basis of a naive dimensional analysis (NDA). However a detailed analysis by Bigi and Uraltsev [18] reports a different value for d_n which equals 1/30 of that of Weinberg's. The big difference between the results of these analyses is an indication of the existence of hadronic uncertainities which are mainly introduced by the matrix elements of O_6 between the nucleon states. In addition to these theoretical uncertainities, we have also problems with experimental data (in that experiment yields only an upper bound on neutron EDM). These can be summarized as

$$d_n^{\rm theor}=c_{\rm theor}\times I_{tb}K(y)10^{-25}e\ {\rm cm}, \tag{27}$$

$$d_n^{\rm actual}=c_{\rm expt}\times d_n^{\rm max}, \tag{28}$$

where $c_{\rm theor}$ and $c_{\rm expt}$ are constants and $|c_{\rm expt}|$ is known to be less than unity. Let us note that $c_{\rm theor}$ is related to the theoretical uncertainities and $c_{\rm expt}$ to the experimental uncertainities. Experiment yields $d_n^{\rm max}=1.1\times10^{-25}e$cm [19]. The function $K(y)$ in (27) is given by [16,17]

$$K(y)=\frac{y}{(y-1)^3}[3/2-2y+y^2/2+\ln(y)]. \tag{29}$$

The common point for the analyses in [17,18] is the presence of the function $K(y)$ which is equal to 1/3 as $y\to1$.

Equating (27) to (28) and defining $\beta=1.1(c_{\rm expt}/c_{\rm theor})$, we obtain

$$I=\beta f(y), \tag{30}$$

where

$$f(y)=\frac{K_{tb}^7(y)}{K(y)}. \tag{31}$$

Note that the constant β in (30) includes now both theoretical and experimental undeterminicies. We shall not make any assumption concerning the value of β; instead we are going to fix it through the use of the experimental results on $b\to s\gamma$ branching ratio.

The $b\to s\gamma$ decay amplitude is given by

$$M=\frac{4G_F}{\sqrt{2}}\frac{\alpha}{4\pi}C_7(\mu)\overline{s(p')}\sigma_{\mu\nu}(m_bR+m_sL)b(p)F^{\mu\nu}, \tag{32}$$

where $C_7(\mu)$ is defined in (8). Using the experimental result on the braching ratio of $b\to s\gamma$ decay [1,2] we get the following circle:

$$(C_7^{\rm SM}+R)^2+I^2=(C_7^{\rm ex})^2, \tag{33}$$

where $C_7^{\rm ex}$ is the experimental value of $C_7(\mu)$

$$0.22\leqslant|C_7^{\rm ex}|\leqslant 0.30. \tag{34}$$

We shall determine the central values of β, r, and A which are defined in Eqs. (20), (16), and (17), respectively. In doing this, we will make use of the circles in Eqs. (18), (20), and (33) together with Eq. (30). Let us note that (30) is obtained by the use of the experimental upper bound on neutron EDM [19], and (33) is constructed with the use of the experimental data on $b\to s\gamma$ branching ratio [1].

Let us first determine β. For this purpose we consider the circle in (33) in the limit of infinitely large M_H or equivalently $y\to 0$. As $y\to 0$, $R\to 0$ and through (30), $I\to\beta f_0$, where numerically $f_0=0.2706$. Then Eq. (33), which is valid for any value of M_H, yields

$$\beta=\pm\left(\frac{(C_7^{\rm ex})^2-(C_7^{\rm SM})^2}{f_0^2}\right)^{1/2}. \tag{35}$$

With (35), I in (30) has now become a completely known function of M_H. Now we solve (33) for R, yielding

$$R=-C_7^{\rm SM}+\sqrt{(C_7^{\rm ex})^2-I^2}, \tag{36}$$

where the choice of plus sign is necessary to satisfy the asymptotic condition on R.

Using (36) for R, and (30) for I we can solve Eq. (18) for r

$$r=1+\frac{(R+R_0)^2+(I+I_0)^2-R_0^2-I_0^2}{t} \tag{37}$$

whose M_H dependence shall be discussed in the next section.

Finally, taking r from (37), R from (36) and I from (30) we determine the CP asymmetry A in (24) whose dependence on M_H shall also be studied in the next section.

III. NUMERICAL ANALYSIS

In the numerical analysis we shall use $m_u=10$ MeV, $m_c=1.5$ GeV, $m_b=4.6$ GeV. For the top quark mass we rely on the CDF data [20] and for the W mass we use $M_W=80.22$ GeV [19].

In calculating I_{tu} and R_{tu} we use the parametrization in [19], and in doing this we take the midvalues of the quantities. For the phase δ_{13} of the CKM matrix in [19] we shall use the the midvalue of $\cos\delta_{13}=0.47\pm 0.32$ given in [21] which icludes a large uncertainity. A straightforward calculation shows that corresponding to the uncertainity in $\cos\delta_{13}$, R_{tu}, and I_{tu} are uncertain by 3.87% and 23.75%, respectively. Thus, the standard model asymmtery A_s in (23) is uncertain by 23.75%, and we shall use its central value in our calculations. This choice is justified by the closeness of I_{tu} and R_{tu} calculated in this way to that obtained by the use of Wolfenstein parametrization [22].

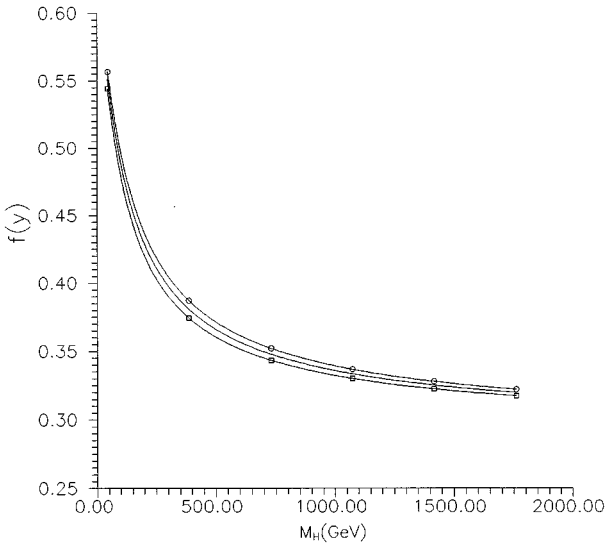

FIG. 1. The M_H dependence of $f(y)$ for $m_t=194$ GeV (with circles), $m_t=176$ GeV (bare solid curve), and $m_t=158$ GeV (with squares).

Figure 1 shows the variation of $f(y)$ in (29) with M_H for the lowest, central, and the highest values of m_t permitted by the CDF data [20]. As we see from Fig. 1 the dependence of $f(y)$ on m_t is very weak; thus, insensitivity of results to the variation of y with m_t is guaranteed. In what follows we shall use therefore the central value of CDF data $m_t=176$ GeV.

For $m_t=176$ GeV we obtain $C_7^{\rm SM}=-0.2686$. The $b\to s\gamma$ branching ratio has approximately 50% error [1] which is transferred into a range of values that $C_7^{\rm ex}$ may take, as described by (34).

With the use of the above-mentioned data we calculate the SM CP asymmetry in (23) to be $A_s=0.0714\%$ in region I, and $A_s=0.0223\%$ in region II.

In the second column of Table I we give the values of β as $|C_7^{\rm ex}|$ moves from its maximum value 0.30 towards $|C_7^{\rm SM}|=0.2686$. We see that $|\beta|$ decreases gradually with decreasing $|C_7^{\rm ex}|$. Moreover, it is seen that the maximum value is $|\beta|\approx 0.5$.

Regarding the present calculations in [17,18] as the possible candidates for $c_{\rm theor}$ in (27), we can make certain predictions for $c_{\rm expt}$ in (28). A simple calculation yields $c_{\rm theor}=9.9$ and $c_{\rm theor}=0.33$ for Weinberg's NDA and Bigi-Uraltsev calculations, respectively. In the case of NDA, a solution for $c_{\rm expt}$ exists only for $|\beta|<\sim 0.27$ at which $d_n^{\rm actual}$ turns out to be very close to its experimental upper bound. On the other hand, for the Bigi-Uraltsev calculation, being a more detailed analysis, for all values of $|C_7^{\rm ex}|$ ranging from $|C_7^{\rm SM}|$ to 0.30 there exists a solution for $c_{\rm ex}$ with the help of which, through (28), one determines the value $d_n^{\rm actual}$. In the third column of Table I we give the values of $d_n^{\rm actual}$ as $|C_7^{\rm ex}|$ moves from its maximum value 0.30 towards $|C_7^{\rm SM}|=0.2686$. We observe that for $|C_7^{\rm ex}|=0.3$, $|d_n^{\rm actual}|$ reaches its maximum value of 1.63×10^{-26} which is 1 order of magnitude less than the present experimental upper bound.

In our numerical analysis we use the range of values of

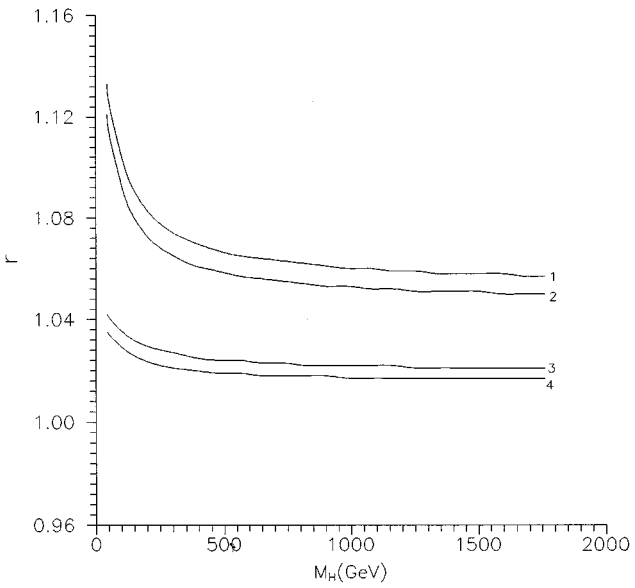

FIG. 2. The M_H dependence of r in region I. Here labels 1, 2, 3, and 4 correspond to $\beta = 0.4938, -0.4938, 0.2922,$ and -0.2922, respectively.

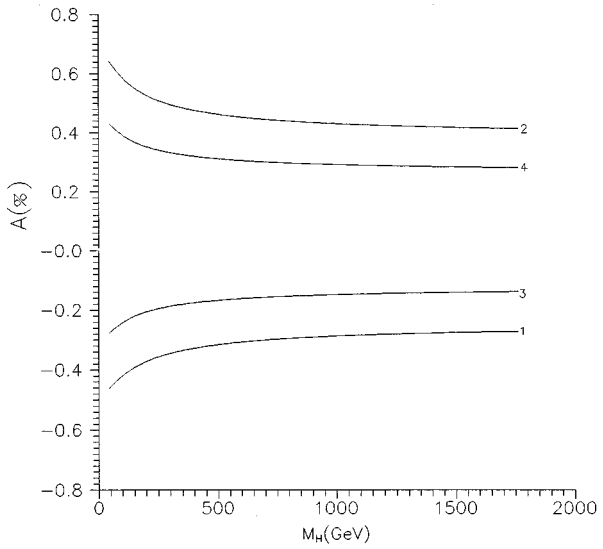

FIG. 4. The M_H dependence of A in region I. Labels have the same meaning as in Fig. 1. Here the unlabeled solid line shows the SM asymmetry.

M_H from 44 GeV [19] to $10m_t$ [16]. In Figs. 2 and 3 we show the variation of r in (37) with M_H in regions I and II, respectively. We observe that in both figures r is fairly high at low M_H and lands rapidly to a lower value after $M_H \sim 500$ GeV.

As we see from Fig. 2, the dependence of r on the sign of β in region I is very weak. Moreover, for $M_H > \sim 1$ TeV, r attains the values ~ 1.056, ~ 1.0050, ~ 1.020, and ~ 1.016 for $\beta = +0.4938$, -0.4938, 0.2922, and -0.2922, respectively.

From Fig. 3 we observe that in region II the dependence of r on the sign of β is large. Specificially, we see that, for large M_H, r becomes practically independent of M_H and attains the values ~ 1.021, ~ 0.998, ~ 1.01, and ~ 0.9996 corresponding to $\beta = +0.4938$, -0.4938, 0.2922, and -0.2922, respectively.

In Figs. 4 and 5 we show the variation of A in (24) with M_H in regions I and II, respectively. What we observe to be common between them is the saturation of CP asymmetry A to a certain value after $M_H \sim 500$ GeV.

From Fig. 4 we observe that the 2HDM CP asymmetry A, practically for all M_H, is of the same order as the SM CP asymmetry A_s. Indeed, especially for large M_H, corresponding to the values of β, $\beta = +0.4938$, -0.4938, 0.2922, and -0.2922, A attains the percentage values of ~ -0.27, ~ 0.40, ~ -0.14, and ~ 0.28.

In Fig. 5 we observe that asymmetry A, as compared to the previous figure, is completey different in that it is positive and takes higher values for all values of M_H. Actually,

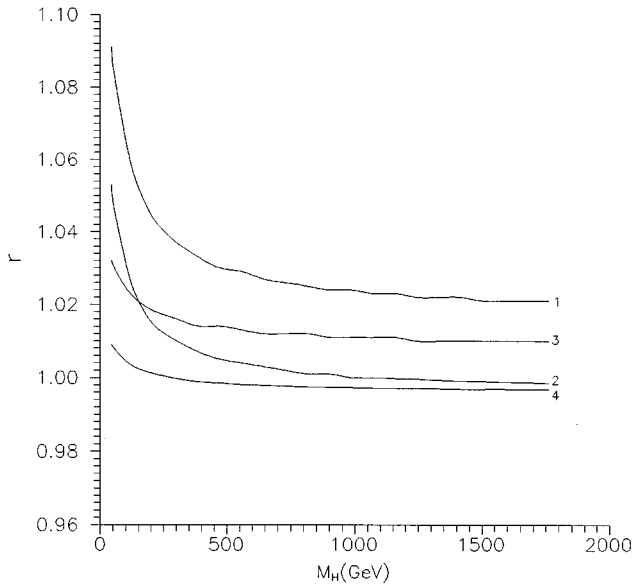

FIG. 3. The same as in Fig. 2 but for region II.

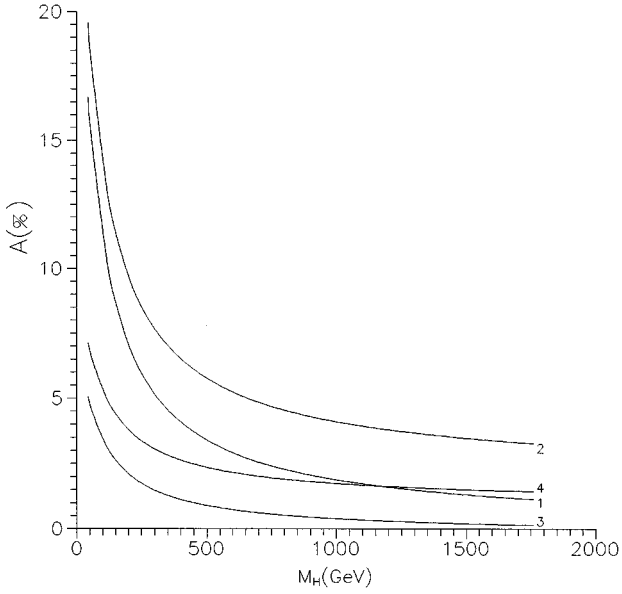

FIG. 5. The same as in Fig. 4 but for region II.

we see that for small M_H, 2HDM CP asymmetry is larger than the SM CP asymmetry by approximately 3 orders of magnitude. For large M_H, however, A gets values which are larger than SM asymmetry by 2 orders of magnitue. Indeed, for large M_H, corresponding to the values of β, $\beta=+0.4938$, -0.4938, 0.2922, and -0.2922, A gets the following percentage values: ~ 1.1, ~ 3.25, ~ 0.2, and ~ 1.5.

The last point to be noted about Figs. 2–5 is that negative β gives rise to larger r and A than positive β does.

To decern a CP asymmetry A at the σ significance level with only statistical errors, the number of B hadrons N_B needed to demonstrate the asymmetry is given by [23]

$$N_B \approx \frac{\sigma^2}{B \times A^2}. \tag{38}$$

Now denoting the number of B hadrons to observe A_s, A in I, and A in II by N_B^s, N_B^{I}, and N_B^{II}, respectively, we get, using the values of r and A we have obtained already, the following ratios:

$$\frac{N_B^{\mathrm{I}}}{N_B^s} \approx 1, \quad \frac{N_B^{\mathrm{II}}}{N_B^s} \approx 10^{-4}, \tag{39}$$

which clearly prove that region II is more suitable for experimental investigations on A.

In conclusion we have determined the 2HDM CP asymmetry A, the ratio of 2HDM decay rate to SM decay rate r, and the actual value of the neutron EDM. In doing these we have utilized the experimental results on the $b \to s\gamma$ branching ratio, and on the upper bound of the neutron EDM. Both r and A relax to constant values after $M_H \sim 500$ GeV. This saturation property of quantities shows that if charged Higgs mass happens to be large (~ 1 TeV) then the most general 2HDM merely shifts the SM values of r and A to some other value which may be important for establishing 2HDM. Boldly speaking, in the high dilepton mass region (region II) r is closer to unity and asymmetry is very large as compared to those in low dilepton mass region (region I). Thus on the basis of the order of magnitude analysis carried out for N_B, we conclude that the high dilepton mass region is important and appropriate for experimental check of the quantities under concern. Region II [6] is accessible to the B experiments which will be carried out with hadron beams in CDF, HERA, and LHC.

TABLE I. Values of β and d_n^{actual} for different values of $|C_7^{\mathrm{ex}}|$.

$\lvert C_7^{\mathrm{ex}}\rvert$	β	$d_n^{\mathrm{actual}}(e-cm)$
0.30	± 0.4938	$\pm 1.63\ 10^{-26}$
0.29	± 0.4040	$\pm 1.33\ 10^{-26}$
0.28	± 0.2922	$\pm 9.65\ 10^{-27}$
0.27	± 0.1015	$\pm 3.35\ 10^{-27}$

[1] R. Ammar *et al.*, Phys. Rev. Lett. **71**, 674 (1993).
[2] B. Barish *et al.*, Phys. Rev. Lett. **74**, 2885 (1995).
[3] A. Buras and M. Munz, Phys. Rev. D **52**, 186 (1994); J. A. Hewett, *ibid.* **53**, 4964 (1996).
[4] L. Wolfenstein, Phys. Rev. D **43**, 151 (1991); N. G. Deshpande *et al.*, *ibid.* **49**, 4812 (1994).
[5] J. M. Soares, Nucl. Phys. **B367**, 575 (1991).
[6] A. Ali *et al.*, Z. Phys. C **67**, 417 (1995).
[7] W.S. Hou and R.S. Willey, Phys. Lett. B **202**, 591 (1988).
[8] Y.L. Wu and L. Wolfenstein, Phys. Rev. Lett. **73**, 1762 (1994).
[9] L. Wolfenstein and Y.L. Wu, Phys. Rev. Lett. **73**, 2809 (1994).
[10] R. Grigjanis *et al.*, Phys. Rev. D **42**, 245 (1990).
[11] P.J. O'Donnell and H.K.K. Tung, Phys. Rev. D **43**, R2067 (1991).
[12] B. Grinstein *et al.*, Nucl. Phys. **B319**, 271 (1989); R. Grigjanis *et al.*, Phys. Lett. B **223**, 239 (1989).
[13] G. Cella *et al.*, Phys. Lett. B **258**, 212 (1991).
[14] M. Ciuchi *et al.*, Phys. Lett. B **316**, 127 (1993); A. Ali *et al.*, *ibid.* **273**, 505 (1991); C.S. Lim *et al.*, *ibid.* **218**, 343 (1989); N.G. Deshpande *et al.*, Phys. Rev. D **39**, 1461 (1989).
[15] N.G. Deshpande *et al.*, Phys. Rev. Lett. **57**, 1106 (1986).
[16] S. Weinberg, Phys. Rev. Lett. **63**, 2333 (1989).
[17] D. Dicus, Phys. Rev. D **41**, 999 (1990).
[18] I.I. Bigi and N.G. Uraltsev, Nucl. Phys. **B353**, 321 (1991).
[19] Particle Data Group, Phys. Rev. D **50**, 1315 (1994).
[20] F. Abe *et al.*, Phys. Rev. Lett. **72**, 2326 (1995).
[21] M. Ciuchini (unpublished).
[22] A. Ali and D. London (unpublished).
[23] J.M. Gerard and W.S. Hou, Phys. Rev. D **43**, 2909 (1991).